


 Cite this: *Chem. Commun.*, 2021, 57, 4958

 Received 30th December 2020,
Accepted 12th April 2021

DOI: 10.1039/d0cc08411e

rsc.li/chemcomm

Formation of phosphine imide (HN=PH₃) and its phosphinous amide (H₂N–PH₂) isomer†

 Cheng Zhu,^{ib} Alexandre Bergantini,^{ib} Santosh K. Singh,^{ab} Ralf I. Kaiser,^{ib} André K. Eckhardt,^{ib} Peter R. Schreiner,^{ib} Ya-Syuan Huang,^d Bing-Jian Sun^d and Agnes H. H. Chang^{*d}

We present the first formation of the previously elusive phosphine imide (HN=PH₃) along with its phosphinous amide (H₂N–PH₂) isomer *via* exposure of phosphine (PH₃) and ammonia (NH₃) ices to ionizing radiation. Our approach may be extended to prepare, separate, and detect highly reactive compounds such as intermediates of Wittig reactions.

Since the pioneering discovery by Hermann Staudinger and Jules Meyer in 1919,¹ iminophosphoranes (R¹N=PR²R³R⁴, where R¹, R², R³, and R⁴ are hydrogen or functional groups) have been widely used as key intermediates in the synthesis of primary amines and amides,^{2–4} chiral nonionic superbases,⁵ electroluminescent materials in organic light emitting diodes (OLEDs),⁶ building blocks for P=N-backbone polymers,⁷ and as ligands for homogeneous catalysis.⁸ Particular attention has been devoted to the prototype of iminophosphorane–phosphine imide (HN=PH₃, **1**) (Fig. 1)–in the theoretical, physical, and synthetic chemistry communities from the fundamental viewpoints of chemical bonding and electronic structure.^{9–15} Electronic structure and charge distribution analyses revealed that the P=N bond of **1** is highly polar, which is similar to the P=O and P=C bonds of its isovalent species phosphine oxide (O=PH₃, **2**) and methylenephosphorane (H₂C=PH₃, **3**), respectively.^{10,12,13,16} The detailed P=X (X=C, N, O) bond properties are still contentious, *e.g.*, a resonance hybrid between a dipolar form and a double bond form, a resonance between single and

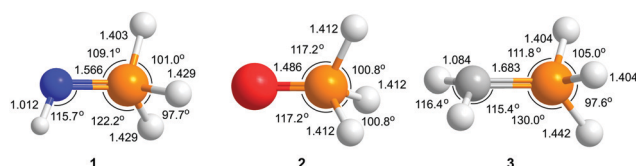


Fig. 1 Computed molecular structures of phosphine imide (HN=PH₃, C_s, **1**), phosphine oxide (O=PH₃, C_{3v}, **2**), and methylenephosphorane (H₂C=PH₃, C_s, **3**) at the B3LYP/cc-pVTZ level of theory (ESI†). The atoms are color coded in white (hydrogen), blue (nitrogen), gray (carbon), red (oxygen), and orange (phosphorous). Bond lengths and angles are given in angstroms and degrees, respectively.

multiple bonds.¹⁶ Comparing **1** to two isomers, phosphinous amide (H₂N–PH₂, **4**)–the mono phosphorus analogue of well-known hydrazine (H₂N–NH₂)–and phosphinoammonium ylide (H₃N=PH, **5**), isomer **1** was computed to be thermodynamically more stable than **5** by 0.55 eV (53 kJ mol^{−1}), but less stable than **4** by 0.97 eV (94 kJ mol^{−1}) (Fig. 2 and ESI†). Nevertheless, a barrier of 2.22 eV (214 kJ mol^{−1}) for the hydrogen shift between **1** and **4** suggests that **1** is kinetically stable and can be identified once synthesized.

However, the experimental preparation and characterization of **1** has remained elusive for more than a century. The Staudinger and Kirsanov reactions are the hitherto most used synthetic methods for the generation of iminophosphoranes (R¹N=PR²R³R⁴) (Scheme 1).^{1,17–22} In the Staudinger reaction, a phosphine (PR²R³R⁴) is oxidized by an organic azide (R¹–N₃) to produce R¹N=PR²R³R⁴,^{1,20,21} which can then be hydrolyzed to primary amines (Staudinger reaction) or react with a variety of electrophiles (aza-Wittig reaction), such as oxiranes, carbon dioxide, carbon disulfide, isocyanates, carbonyl compounds to produce aziridines, isocyanates, isothiocyanates, carbodiimides, and imines, respectively (Scheme 1).^{2,4} When R¹–N₃ are not available, R¹N=PR²R³R⁴ can also be prepared by bromination of PR²R³R⁴ to bromophosphonium bromide (R²R³R⁴PBr⁺Br[−]) and *in situ* treatment of the salt with alkylamines (R¹–NH₂) (Kirsanov reaction).^{17,19,22} However, the simplest iminophosphorane

^a Department of Chemistry, University of Hawaii at Manoa, 2545 McCarthy Mall, Honolulu, HI 96822, USA

^b W. M. Keck Laboratory in Astrochemistry, University of Hawaii at Manoa, 2545 McCarthy Mall, Honolulu, HI 96822, USA. E-mail: ralfk@hawaii.edu

^c Institute of Organic Chemistry, Justus Liebig University, Heinrich-Buff-Ring 17, Giessen 35392, Germany. E-mail: ake05@mit.edu

^d Department of Chemistry, National Dong Hwa University, Shoufeng, Hualien 974, Taiwan. E-mail: hhchang@gms.ndhu.edu.tw

† Electronic supplementary information (ESI) available. See DOI: 10.1039/d0cc08411e

‡ Present address: Centro Federal de Educacao Tecnologica Celso Suckow da Fonseca - CEFET/RJ, Av. Maracana 229, 20271-110, Rio de Janeiro (Brazil).

§ Present address: MIT Department of Chemistry, Cambridge, MA 02139 (USA).

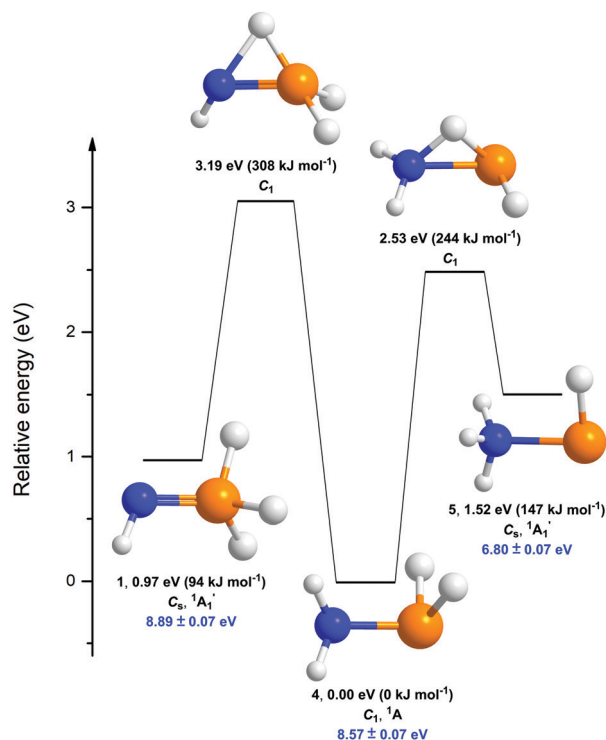
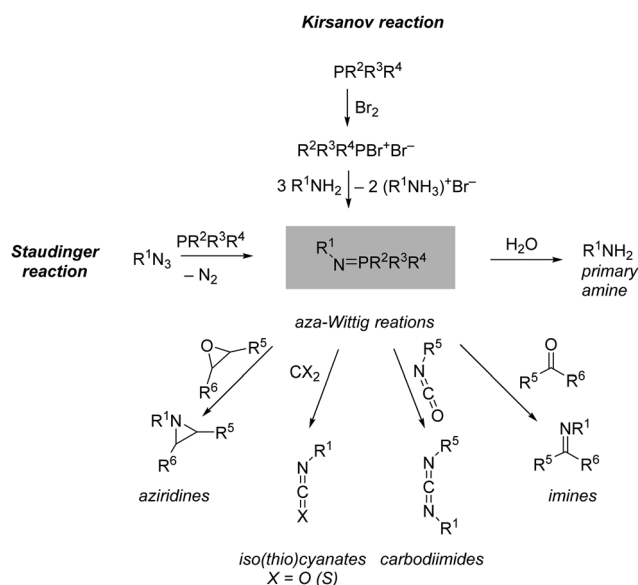


Fig. 2 Potential energy surface for the isomerization of NPH_4 isomers at CCSD(T)/CBS//B3LYP/cc-pVTZ including zero-point vibrational energy (ZPVE). Relative energies, point groups, ground electronic states, and computed adiabatic ionization energies corrected for the electric field effect (-0.03 eV, Stark effect, ESI †) (blue) are also shown (ESI †). The atoms are color coded in white (hydrogen), blue (nitrogen), and orange (phosphorous).



Scheme 1 Typical synthetic routes and applications for iminophosphoranes.

$\text{HN}=\text{PH}_3$ still has not been reported even though the precursors for conventional Staudinger and Kirsanov reactions, *e.g.*, phosphine (PH_3), hydrogen azide (HN_3), and ammonia (NH_3), are easy to obtain.

Here we report the first preparation and detection of **1** as well as its isomer **4** by exposing low temperature ice mixtures of PH_3 and NH_3 to energetic electrons (Table S1, ESI †). Both isomers were unambiguously identified during warming the electron processed ices from 10 K to 300 K at a rate of 1 K min^{-1} (temperature-programmed desorption (TPD)) by selectively photoionizing the isomer based on their ionization energies exploiting tunable vacuum ultraviolet (VUV) single-photon ionization reflectron time-of-flight mass spectrometry (PI-ReTOF-MS). Besides the characterization of the previously absent **1**, our novel route may be extended to form their isoalent species, *e.g.*, 3—the simplest ylide in, *e.g.*, Wittig reactions—which to the best of our knowledge has not been reported either.

Fourier-Transform Infrared spectroscopy (FTIR) was utilized to monitor the chemical evolution of the phosphine–ammonia ices induced by the electron processing at 5 K (Fig. S1 and Tables S2, S3, ESI †). The irradiation process decomposed $5 \pm 1\%$ of phosphine and ammonia producing new absorptions of $\nu_{\text{P}=\text{N}}$ (1100 and 1153 cm^{-1}), ν_{NH_2} (ν_2 , 1508 cm^{-1}), $\nu_{\text{N}=\text{N}}$ (2090 cm^{-1}), $\nu_{\text{P}-\text{H}}$ (2238 cm^{-1}), $\nu_{\text{N}=\text{NH}_2}$ (ν_5 , 2785 cm^{-1}), and $\nu_{\text{N}-\text{H}}$ (3165 and 3330 cm^{-1}).^{23–27} Substitution of ammonia (NH_3) by ^{15}N -ammonia ($^{15}\text{NH}_3$) shifted the bands of nitrogen-bearing functional groups to lower wavenumbers, which supports the previous assignments (Tables S2 and S3, ESI †). The identification of new P=N, P-H, and N-H absorptions could be partly due to the formation of PNH_4 isomers. However, since electron irradiation can produce a significant array of new species and isomers with close vibrational absorptions,²⁷ in complex mixtures, infrared spectroscopy is able to determine predominantly newly formed *functional groups*, but does not allow the identification of *individual isomers*. Therefore, an alternative method was required to identify individual isomers.

After the irradiation, the ice was warmed at a rate of 1 K min^{-1} to 300 K; PI-ReTOF-MS was exploited to analyze the sublimed species from the ice.^{28,29} This method can discriminate isomers by systematically tuning the ionization photon energies to *selectively ionize* the desorbed species without fragmentation based on their adiabatic ionization energies (IEs) and then mass resolving the generated molecular ions with the ReTOF-MS. Photon energies of 10.49 eV, 9.43 eV, 8.80 eV, and 8.20 eV were selected based on the computed IEs of the PNH_4 isomers (Fig. 2 and Table S4, ESI †). Vacuum ultraviolet (VUV) photons with energies of 10.49 eV and 9.43 eV are able to ionize all isomers (**1**, **4**, **5**); 8.80 eV photons can ionize **4** (IE = 8.57 eV), **5** (IE = 6.80 eV), whereas 8.20 eV photons can only ionize **5**. Comparison of the signals of the molecular ions PNH_4^+ ($m/z = 49$) at these PI energies could lead to the discrimination of the isomers. Fig. 3 compiles the mass spectra of the desorbed molecules from the electron processed ices; the corresponding TPD profiles of the target ions PNH_4^+ are visualized in Fig. 4.

In detail, for the PH_3/NH_3 system, the signal at $m/z = 49$ exhibits a broad sublimation feature with a maximum at 125 K extending from 110 to 160 K at a photon energy of 10.49 eV (Fig. 4(a)). In a separate experiment using ^{15}N substituted nitrogen ($\text{PH}_3/^{15}\text{NH}_3$ system), the peak shifted by 1 amu to

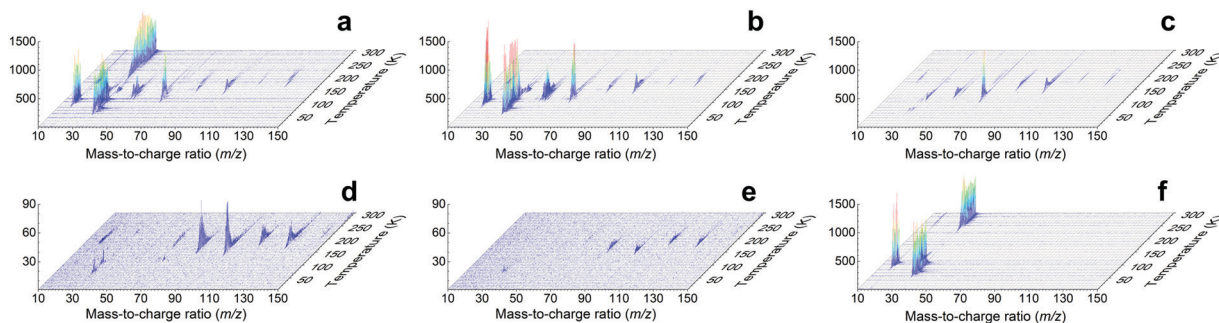


Fig. 3 PI-ReTOF-MS data during the temperature programmed desorption (TPD) phase of the electron processed ices at distinct photon energies. (a), 10.49 eV, phosphine (PH₃)/ammonia (NH₃). (b), 10.49 eV, phosphine (PH₃)/¹⁵N-ammonia (¹⁵NH₃). (c), 9.43 eV, phosphine (PH₃)/ammonia (NH₃). (d), 8.80 eV, phosphine (PH₃)/ammonia (NH₃). (e), 8.20 eV, phosphine (PH₃)/ammonia (NH₃). (f), 10.49 eV, phosphine (PH₃)/ammonia (NH₃) ice without electron irradiation.

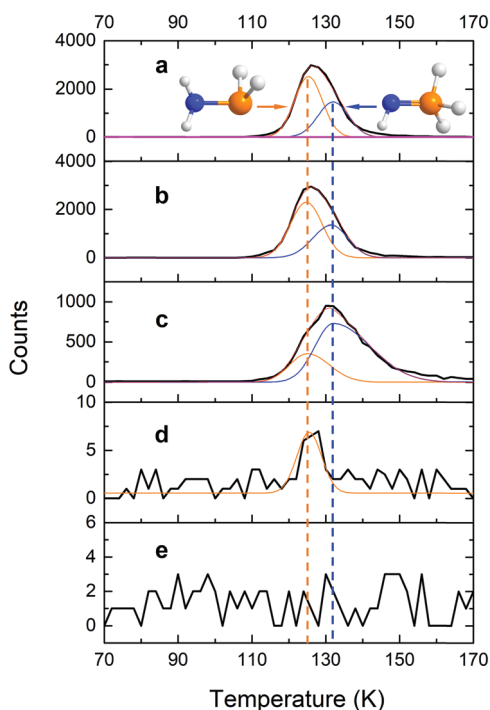


Fig. 4 PI-ReTOF-MS data during the temperature programmed desorption (TPD) phase of the electron processed ices at distinct photon energies. (a), 10.49 eV, $m/z = 49$, phosphine (PH₃)/ammonia (NH₃). The magenta line shows the $m/z = 49$ signal extracted from the data of blank experiment (no electron irradiation). (b), 10.49 eV, $m/z = 50$, phosphine (PH₃)/¹⁵N-ammonia (¹⁵NH₃). (c), 9.43 eV, $m/z = 49$, phosphine (PH₃)/ammonia (NH₃). (d), 8.80 eV, $m/z = 49$, phosphine (PH₃)/ammonia (NH₃). (e), 8.20 eV, $m/z = 49$, phosphine (PH₃)/ammonia (NH₃).

$m/z = 50$ (Fig. 4(b)). These results indicate that the carriers of the $m/z = 49$ signals contain one nitrogen atom and therefore can only be PNH₄ isomers. When the photon energy was lowered to 9.43 eV, the sublimation profile shows a peak at 132 K with a shoulder at 125 K (Fig. 4(c)). These results indicate that there should be two sublimation events at 125 K and 132 K. By deconvoluting the TPD profile with bimodal Gaussian mixture model,^{30–32} the ratio of the integrated areas of the two sublimation events at 125 K and 132 K is determined to be

(0.4 ± 0.1):1 (Table S5, ESI[†]). Deconvolution of the profile at PI = 10.49 eV reveals a 125 K to 132 K ratio of (1.6 ± 0.1):1, which is significantly higher than that at PI = 9.43 eV; therefore, both peaks are linked to distinct PNH₄ isomers as photoionization cross sections for different isomers vary with respect to photon energies;³³ if both sublimation events are linked to the same isomer, the ratios of the integrated ion counts of the sublimation profiles at 125 K and 132 K should be identical at the 10.49 eV and 9.43 eV experiments. Having provided evidence on the existence of two distinct PNH₄ isomers, we decreased the photon energy further. By tuning down the photon energy to 8.80 eV, the first peak at 125 K is still present, while the second sublimation event at 132 K vanishes (Fig. 4(d)). This reveals that the sublimation event at 132 K must be associated with a PNH₄ isomer, which cannot be ionized with 8.80 eV photons. At 8.80 eV, isomers 4 (IE = 8.57 eV) and 5 (IE = 6.80 eV) can still be ionized; therefore, the low temperature sublimation event is associated with isomer 4 (IE = 8.57 eV) and/or 5 (IE = 6.80 eV); the sublimation event at 132 K can only be assigned to 1 (IE = 8.89 eV). Further lowering the photon energy to 8.20 eV eliminates the 125 K peak (Fig. 4(e)). At this photon energy, isomer 5 (IE = 6.80 eV) should be ionized. Therefore, the 125 K peak is linked to 4. Note that the most thermodynamically unfavorable isomer 5 was not detected. We also carried out experiments under the same conditions but without electron irradiation of the ices and did not detect ion counts at these m/z ratios (Fig. 4(a)) confirming that the identified species are due to electron processing the ices, but not from contaminations or direct reactions of the precursors.

Having identified PNH₄ isomers 1 and 4, we shift our attention to untangling their possible formation pathways based on the experiments exploiting heavy ammonia (ND₃) and PH₃ (Fig. S2–S4 and Table S5, ESI[†]). Upon interaction with energetic electrons, ND₃ decomposes to *n*-amino radical ([•]ND₂) plus suprathreshold atomic deuterium (D) and to *n*-imidogen ([[•]ND] diradical plus molecular deuterium (D₂) (Fig. S4, ESI[†]).^{26,34} The PH₃ precursor undergoes decomposition to the phosphino radical ([•]PH₂) plus suprathreshold hydrogen and phosphinidene ([[•]PH] plus molecular hydrogen.³⁵ Two mechanisms can lead to the formation of the PNH₄ isomers: radical-radical (amino/phosphino)

recombination and insertion/addition reactions (imidogen/phosphinidene). If the $\bullet\text{ND}_2$ and $\bullet\text{PH}_2$ radicals hold favorable recombination geometries, they can recombine barrierlessly to form $\text{D}_2\text{N-PH}_2$ (**4**, 51 amu) followed by potential (partial) isomerization to $\text{DN=PH}_2\text{D}$ (**1**, 51 amu) and/or $\text{D}_2\text{HN=PH}$ (**5**, 51 amu). On the other hand, if $|\dot{\text{P}}\text{H}$ and $|\dot{\text{N}}\text{D}$ species are in the first excited singlet state ($a^1\Delta$),^{35,36} they are able to insert into the N–D bonds of ND_3 and P–H bonds of PH_3 , respectively, producing $\text{D}_2\text{N-PHD}$ (**4**, 52 amu) and HDN-PH_2 (**4**, 50 amu), respectively. The former species $\text{D}_2\text{N-PHD}$ (**4**, 52 amu) may isomerize to DN=PHD_2 (**1**, 52 amu) and/or $\text{D}_3\text{N=PH/D}_2\text{HN=PD}$ (**5**, 52 amu). The latter one HDN-PH_2 (**4**, 50 amu) may isomerize to $\text{HN=PDH}_2/\text{DN=PH}_3$ (**1**, 50 amu) and/or $\text{H}_2\text{DN=PH}$ (**5**, 50 amu). The $|\dot{\text{P}}\text{H}$ and $|\dot{\text{N}}\text{D}$ species could also add to the non-bonding electron pair of ND_3 and PH_3 generating $\text{D}_3\text{N=PH}$ (**5**, 52 amu) and DN=PH_3 (**1**, 50 amu), respectively. The ratio of the ion counts for $m/z = 51:(50 + 52)$ is calculated to be $(1.6 \pm 0.2):1$ (Table S5, ESI[†]). This finding suggests that the radical–radical recombination between $\bullet\text{ND}_2$ and $\bullet\text{PH}_2$ is favorable considering the preferential formation of $\bullet\text{ND}_2$ and $\bullet\text{PH}_2$ radicals compared to $|\dot{\text{N}}\text{D}$ and $|\dot{\text{P}}\text{H}$.^{26,35} Note that we do not exclude isotope scrambling between PH_3 and ND_3 and therefore cannot explicitly distinguish the two possible (or any alternative) routes.

In summary, our study provides compelling evidence for the first preparation of phosphine imide (HN=PH_3 , **1**) along with its isomer phosphinous amide ($\text{H}_2\text{N-PH}_2$, **4**) via energetic electrons processing of phosphine and ammonia ice mixtures. The isomers were identified in the sublimed molecules during warming the ices exploiting tunable vacuum ultraviolet single-photon photoionization reflectron time of flight mass spectrometry (PI-ReTOF-MS). The distance between the photoionization laser and the ice surface is 2 mm. The average velocity of the two isomers subliming in the 110 to 160 K range is determined to be 260 m s^{-1} . Therefore, to survive from sublimation to photoionization events, the lifetimes of phosphine imide and phosphinous amide have to be at least $7 \mu\text{s}$. This work offers a possible method and mechanistic framework to prepare and discriminate highly reactive molecules and their isomers, such as critical intermediates of Wittig reactions (methylenephosphorane ($\text{H}_2\text{C=PH}_3$, **3**)) and hetero-Wittig reactions.

This work was supported by NASA under Grant NNX16AD27G to Hawaii (R. I. K.). The equipment was financed by the W. M. Keck Foundation. The data analysis and preparation of the manuscript was partially financed by the Alexander von Humboldt Foundation (Feodor Lynen research fellowship; A. K. E.). Y.-S. H., B.-J. S., and A. H. H. C. thank the National Center for High-performance Computer in Taiwan for providing the computer resources in the calculations.

Conflicts of interest

There are no conflicts of interest to declare.

Notes and references

- 1 H. Staudinger and J. Meyer, *Helv. Chim. Acta*, 1919, **2**, 635–646.
- 2 F. Palacios, C. Alonso, D. Aparicio, G. Rubiales and M. Jesús, *Tetrahedron*, 2007, **63**, 523–575.
- 3 G. Hajos and I. Nagy, *Curr. Org. Chem.*, 2008, **12**, 39–58.
- 4 A. R. Katritzky, *Advances in heterocyclic chemistry*, Academic Press, California, 1995.
- 5 P. Ilankumaran, G. Zhang and J. G. Verkade, *Heteroat. Chem.*, 2000, **11**, 251–253.
- 6 S. Višniakova, I. Urbanavičiūtė, L. Daukšaitė, M. Janulevičius, B. Lenkevičiūtė, I. Sychugov, K. Arlauskas and A. Žilinskas, *J. Lumín.*, 2015, **167**, 261–267.
- 7 V. Blackstone, A. J. Lough, M. Murray and I. Manners, *J. Am. Chem. Soc.*, 2009, **131**, 3658–3667.
- 8 J. García-Álvarez, S. E. García-Garrido and V. Cadierno, *J. Organomet. Chem.*, 2014, **751**, 792–808.
- 9 P. V. Sudhakar and K. Lammertsma, *J. Am. Chem. Soc.*, 1991, **113**, 1899–1906.
- 10 L. Nyulaszi, T. Veszpremi and J. Reffy, *J. Phys. Chem.*, 1995, **99**, 10142–10146.
- 11 J. Koketsu, Y. Ninomiya, Y. Suzuki and N. Koga, *Inorg. Chem.*, 1997, **36**, 694–702.
- 12 C. Widauer, H. Grützmacher, I. Shevchenko and V. Gramlich, *Eur. J. Inorg. Chem.*, 1999, 1659–1664.
- 13 D. Chesnut and A. Savin, *J. Am. Chem. Soc.*, 1999, **121**, 2335–2336.
- 14 I. Alkorta, G. Sánchez-Sanz, J. Elguero and J. E. D. Bene, *J. Phys. Chem. A*, 2014, **118**, 1527–1537.
- 15 T. Yang, D. M. Andrada and G. Frenking, *Mol. Phys.*, 2019, **117**, 1306–1314.
- 16 D. G. Gilheany, *Chem. Rev.*, 1994, **94**, 1339–1374.
- 17 S. Eguchi, Y. Matsushita and K. Yamashita, *Org. Prep. Proced. Int.*, 1992, **24**, 209–243.
- 18 A. W. Johnson, K. A. Starzewski and W. C. Kaska, *Ylides and Imines of Phosphorus*, Wiley, New York, 1993.
- 19 A. Buchard, H. Heuclin, A. Auffrant, X. F. Le Goff and P. Le Floch, *Dalton Trans.*, 2009, 1659–1667.
- 20 S. S. Van Berkel, M. B. Van Eldijk and J. C. Van Hest, *Angew. Chem., Int. Ed.*, 2011, **50**, 8806–8827.
- 21 Y. G. Gololobov and L. F. Kasukhin, *Tetrahedron*, 1992, **48**, 1353–1406.
- 22 T. Rodima, V. Mäemets and I. Koppel, *Perkin 1*, 2000, 2637–2644.
- 23 T. Shimanouchi, *J. Phys. Chem. Ref. Data*, 1977, **6**, 993–1102.
- 24 J. H. Teles, G. Maier, B. Andes Hess Jr and L. J. Schaad, *Chem. Ber.*, 1989, **122**, 749–752.
- 25 G. Socrates, *Infrared and Raman Characteristic Group Frequencies*, John Wiley & Sons, Ltd, New York, 3rd edn, 2004.
- 26 W. Zheng, D. Jewitt, Y. Osamura and R. I. Kaiser, *Astrophys. J.*, 2008, **674**, 1242.
- 27 A. M. Turner, M. J. Abplanalp, S. Y. Chen, Y. T. Chen, A. H. Chang and R. I. Kaiser, *Phys. Chem. Chem. Phys.*, 2015, **17**, 27281–27291.
- 28 B. M. Jones and R. I. Kaiser, *J. Phys. Chem. Lett.*, 2013, **4**, 1965–1971.
- 29 C. Zhu, A. K. Eckhardt, A. Bergantini, S. K. Singh, P. R. Schreiner and R. I. Kaiser, *Sci. Adv.*, 2020, **6**, eaba6934.
- 30 T. Yu and H. Peng, *Am. Sci.*, 2010, **11**, 559.
- 31 P. Kuzema, O. Stavinskaya, I. Laguta and O. Kazakova, *J. Therm. Anal. Calorim.*, 2015, **122**, 1231–1237.
- 32 S. Chernyak, A. Ivanov, N. Strokova, K. Maslakov, S. Savilov and V. Lunin, *J. Phys. Chem. C*, 2016, **120**, 17465–17474.
- 33 L. Zhao, R. I. Kaiser, B. Xu, U. Ablikim, M. Ahmed, M. M. Evseev, E. K. Bashkurov, V. N. Azyazov and A. M. Mebel, *Nat. Astron.*, 2018, **2**, 973–979.
- 34 M. Förstel, Y. A. Tsegaw, P. Maksyutenko, A. M. Mebel, W. Sander and R. I. Kaiser, *ChemPhysChem*, 2016, **17**, 2726–2735.
- 35 A. M. Turner, M. J. Abplanalp and R. I. Kaiser, *Astrophys. J.*, 2016, **819**, 97.
- 36 T. Fueno, V. Bonacic-Koutecky and J. Koutecky, *J. Am. Chem. Soc.*, 1983, **105**, 5547–5557.